

MNRAS, submitted

# QUASAR-GALAXY INTERACTIONS: A POSSIBLE MECHANISM OF FORMATION OF CD-GALAXIES AND GRAVITATIONAL LENSES.

J.ANOSOVA<sup>1</sup>, P.M.S.NAMBOODIRI<sup>2</sup> &

M.R.DESHPANDE<sup>1</sup>

FERMILAB

<sup>1</sup> Physical Research Laboratory, Ahmedabad, India; Phys. Res. Lab.

<sup>2</sup> Indian Institute of Astrophysics, Bangalore, India Indian Inst. Astrophys.

NOV 21 1994

LIBRARY

## Abstract.

Tidal effects of disruption and merger, within a system consisting of a massive quasar and a galaxy cluster, have been studied by computer simulations using Aarseth's NBODY2 code. The model consists of a spherical N-body galaxy cluster and a point-mass quasar. A wide range of initial conditions (ratios of masses of objects, the virial coefficient  $q$  of the N-body system, the pericentric distance of the initial quasar/cluster orbit) has been used.

It is shown that, for small pericentric distances of the initial parabolic orbit of the quasar, and for values of the virial coefficient  $q$  greater than 0.5, collisions of objects can result in their merger, and the formation of products with properties of cD-galaxies or gravitational lenses.

During the evolution of the system, especially after collisions, there are many close and wide binary and multiple galaxies, some containing the quasar and some without it. In the latter case, as a rule, binary galaxies are very close, and the components are preferentially from the larger masses of the initial mass distribution.

**Keywords:** interacting galaxies - quasars, galaxy clusters - cD-galaxy - gravitational lenses

FPRINT-94-65  
5 226500 0911  
0 1160 0053623

## I. Introduction

Interacting galaxies are some of the remarkable objects in the Universe. Many authors try to explain properties of these galaxies by studying the dynamics with N-body computer simulations. Numerical investigations in this field were first performed by Toomre and Toomre (1972). At present there are several reviews of such investigations: see for example Barnes & Hernquist (1992), and the references therein. White (1983) summarized earlier numerical work in this field. Schweizer (1986) summarized the observational properties of galactic collisions. Many investigations of interacting galaxies have been presented in two recent International Conferences, edited by Sulentic et al. (1990) and by Wielen (1990).

A model of the collision of two galaxies where the first one is a massive smoothed particle and the second an N-body system has been used by several authors for many years (e.g. Namboodiri & Kochhar 1993, and references therein). Many effects of collisions of these objects, such as disruption of the N-body cluster, tidal effects, formation of bridges and tails between the galaxies, and the structure of the surface density profile of the remnant, have been considered by these authors. In this paper, we use the same model for the investigation of tidal effects (disruption and merger) of a massive perturber, a quasar, on a galaxy cluster (the N-body system).

Observations of quasars with low redshifts show that 70% or more of these objects have nearby companions (French & Gunn 1983; Heckman et al. 1984; Vader et al. 1987; Hutchings et al. 1989). Sometimes tidal tails and bridges are observed between them (Stockton 1978; MacKenty & Stockton 1984; Stockton & MacKenty 1987; Hutchings et al. 1988; Block & Stockton 1991; Stockton & Ridgway 1991). A distinctive feature of large clusters of galaxies is the presence of one or two highly luminous supergiant elliptical galaxies near the centres of the clusters. These galaxies, known as cD galaxies, are the most luminous galaxies in the universe and have extended amorphous stellar envelopes; they are the most massive stellar systems with masses of about  $10^{12} M_{\odot}$  (Matthews, Morgan & Schmidt 1964; Morgan & Lesh 1965; Tonry 1987; Tremaine 1990). The potential associated with cores of clusters that contain cD-galaxies is 10 times deeper than that associated with normal galaxies; about 80% of these galaxies are located at surface density maxima. The envelopes of cD-galaxies may consist of debris stripped from cluster galaxies by the tidal field of a cluster or by collisions with other galaxies. Particles in such envelopes have a smaller velocity dispersion (about 300 km/s) than that of the cluster (about 800 km/s) – Tonry (1984, 1985); Smith et al. (1985), and references therein.

Since cD galaxies give out a large amount of energy it is worthwhile to establish the radiation mechanism and the physical processes leading to the excess energy generation. About 50% of cD-galaxies have close secondary companions or multiple nuclei. Sometimes we observe dumbbell cD-galaxies with small separations between components, small differences of their magnitudes, and small rms velocities. The Coma cluster is an example of a galaxy cluster containing a dumbbell with two cD-galaxies.

There are many arguments that the brightest IRAS galaxies will evolve into quasars (Sanders et al. 1990), and that they are associated with mergers. There is also indirect evidence that quasar activity is triggered by galaxy collisions. Studies (see for example Gehren et al. 1984; Hutchings et al. 1984; Malkan et al. 1984; Smith et al. 1986) of the morphological structure of quasar hosts show that most of these galaxies are disturbed. Several authors (Negroponte & White 1983; Noguchi 1988; Barnes & Henquist 1991) have examined with computer simulations the possibility that tidal forces can drive gas into the nuclei of interacting galaxies. But there are some difficulties with any explanation of the properties of these objects.

Many investigators have discussed possible mechanisms for the formation of cD-galaxies. Such mechanisms could be:

1. hierarchical clustering, in which dissipation and pressure concentrate the luminous material in dense cores with small radii (a collapse), and halos that have been disrupted (White & Rees 1978; White 1978, and references therein);
2. mergers in small galaxy groups (galaxy-galaxy collisions);
3. a series of mergers among giant galaxies of the cluster;
4. clusters containing two cD-galaxies are the product of a merger of two clusters; each of them contained a central luminous cD-galaxy;
5. mergers of two galaxy subclusters.

But all such models cannot give a satisfactory explanation of all characteristics of cD-galaxies in rich clusters (see Tremaine 1990). Our main aim is to determine initial conditions for a model of 'quasar/galaxy-cluster interaction' which will yield a final remnant with the properties of cD-galaxies. An explanation of the formation of these objects would be very important for our understanding of many processes involved in the formation of spatial structure in the Universe (see for example recent reviews by Tremaine 1990, Barnes & Hernquist 1992, and references therein).

In this paper, we study tidal effects of the collision of a quasar with a galaxy cluster. A quasar is treated as a smoothed particle; a galaxy cluster is treated as a spherical

N-body system, and the individual galaxies have different masses. We study collisions of these objects by computer simulations using Aarseth's NBODY2 code. We consider a wide range of initial conditions in which a quasar and cluster approach each other on parabolic orbits. We change the pericentric distance of the relative orbit of the objects, the mass of the quasar, and the initial parameters of the cluster.

We notice that when the pericentric distance is small, and the mass of the quasar and the virial coefficient  $q$  of the cluster are large, the collision results in a merger. For all models, about 30% of particles escape from the full system, other particles having been captured by the quasar. For our model with largest initial virial coefficient,  $q_0 = 0.90$ , the final product has many properties of cD-galaxies. For large mass of quasar, we obtain remnants with structure like that of clusters of galaxies with gravitational lenses. In these cases, the final remnant is a quasar surrounded by numerous faint dwarf galaxies; these galaxies form long arcs with large curvature and tangential elongations around the quasar. The properties of gravitational lenses have been summarized by Blandford & Narayan (1992).

In the final stage of all models under consideration quasars form close binaries with faint galaxies. In our model with smallest initial virial coefficient,  $q_0 = 0.25$ , we found the formation of a quadruple system which consists of the quasar and three light galaxies.

After the collision of a quasar and a galaxy cluster we observe many multiples (as a rule, triples) which contain a quasar and faint galaxies. These multiples have negative total energies. As the result of strong close interactions of a few galaxies (in particular, triple or quadruple interactions), these multiples form and quickly disrupt. For all models, we obtain also many close temporary and final multiples with high-mass galaxies at various distances from the quasar.

## 2. Method and initial conditions

We consider the following model of the interaction of a quasar with a galaxy cluster. A quasar is a 'softened' point mass  $M$ ; a galaxy cluster is a spherical 250-body system with individual galaxies having different masses. We study collisions of these objects by computer simulations using Aarseth's NBODY2 code. We consider a wide range of initial conditions for the approach of the quasar and the cluster on parabolic orbits. We change the pericentric distance  $p$  of the relative orbit, the mass of the quasar, and the initial parameters of the cluster. A cluster of galaxies with a total mass  $M_1$  is taken. This cluster is a spherical system of 250 particles distributed randomly.

We integrate numerically the equations of motion of the 251 particles using Aarseth's NBODY2 code. A softened potential  $F_i$  for each particle has been used which is given by

$$F_i = -G \sum \frac{m_i}{\sqrt{r_{ij}^2 + s^2}} , \quad (1)$$

where  $G$  is the gravitational constant,  $i, j=1, 2, \dots, 251$ ,  $m_i$  are the masses,  $r_{ij}$  are distances between these particles, and  $s$  is the softening parameter.

We use a system of units with  $G = 1$ , the total mass of the cluster is  $M1 = 1$ , and the total energy of the cluster is  $E = -0.25$  (see Namboodiri and Kochhar 1990). We take the value of the softening parameter to be  $s = 0.1R$  where  $R$  is the initial radius of the cluster. In a physical system of units, if we assume that the most massive galaxy in the cluster is  $10^{11} M_\odot$ , and that the cluster radius  $R = 1 \text{ Mpc}$ , then the unit of time is approximately  $10^9 \text{ yr}$ .

Initial positions of the  $N$  particles are chosen randomly inside a sphere of a radius  $R$ . Initial velocity magnitudes  $V_0$  are taken from the interval  $[-1, +1]$ . Values of  $V_0$  are then normalized by the condition

$$q_0 = T_0/(-U_0) , \quad (2)$$

where  $q_0$ ,  $T_0$ , and  $U_0$  are the initial virial coefficient, and the kinetic and potential energies of the cluster respectively. Directions of velocity vectors of the particles are chosen randomly. Such a cluster has initially a small angular momentum.

We consider different values of the initial virial coefficient  $q_0$ . We use the following method of choosing masses for the particles of a cluster. In a cluster there are five groups of masses, presented in Table Ia. In this Table  $N_{gr}$  is the number of the group of masses;  $n$  is the number of bodies in the group,  $m$  is the mass of a particle, and  $\Sigma m$  is the total mass of the group. This method of choosing the mass gives a distribution of masses which is close to that inferred from the observed distribution of luminosities of galaxies (Schechter, 1980).

A wide range of initial conditions (ratio of mass of quasar to cluster, initial virial coefficient  $q_0$  of the cluster, and pericentric distance  $p$  of the orbit) have been used. We consider 10 models with various initial parameters given in Table I. This table presents the values of  $q_0$ ,  $p$ ,  $M$ ,  $\delta_F$ , and the serial number  $N_0$  of the model, as well as  $d_0$  and  $t_f$ , where  $d_0$  is the initial separation between quasar and cluster, and  $t_f$  is the final moment of the calculation.  $\delta_F$  is the ratio of tidal and gravitational forces of the system (quasar

and galaxy cluster):

$$\delta_F = \frac{GM}{M1} \left( \frac{R_0}{d_0} \right)^3, \quad (3)$$

where  $M1$  and  $R_0$  are the mass and initial radius of the cluster. Asterisks indicate models with retrograde initial motions of the cluster and the quasar (see below).

The initial separation  $d_0$  of the quasar and cluster is chosen so that  $d_0/p$  is in the range 2 to 10. The values of  $p$  and  $d_0$  are given in Table I. The orbital plane is chosen to be the XY plane with the X-axis pointing in the direction of closest approach. The initial relative velocity of the quasar appropriate to its distance  $d_0$  is determined from the standard point-mass formula. It should be noted that soft-potential orbits are not exactly conic sections.

The positions and velocities of the bodies in the cluster and of the quasar were recalculated with reference to the centre-of-mass frame of the total system. The evolution of the cluster is followed until the quasar reaches a distance  $d > 2p$ . We consider two types of relative parabolic motion of the quasar and the centre of mass of the cluster: 1) prograde motion when the ‘quasar-cluster’ binary and the cluster rotate in the same directions; 2) retrograde motion, where these directions are opposite. In Table I the latter models are denoted by asterisks.

### 3. Results of computer simulations

The results of the simulations are stored after specific intervals of time. The centre of mass of the particles (excluding the quasar) is computed after each time interval, and particles with positive energy with respect to this centre of mass are identified as escapers. The centre of mass of the remaining particles is again evaluated and the escapers relative to the new centre of mass are again identified. This procedure is continued until convergence is reached. In this way, we define the number of escapers, the number of bound particles with respect to the cluster, and the evolutionary characteristics of clusters (Namboodiri & Kochhar 1990; 1991a, b; 1993).

Table II shows the maximum relative changes of values of evolutionary parameters of a cluster during its evolution:  $\delta_E$  is the maximum relative change of the total energy  $E$ ,

$$\delta_E = |(E_{max} - E_{min})/E_{min}|, \quad (4)$$

where  $E_{max}$ ,  $E_{min}$  are the maximum and minimum of the energy of the cluster during the period  $t_f$  of evolution. We similarly define  $\delta_L$  as the maximum change of the angular

momentum  $L$ ,  $\delta_q$  as the change of the virial coefficient  $q$ ,  $\delta \langle R \rangle$  and  $\delta(R_m)$  as changes of the average distance and maximum distance of the  $N$  particles from the centre of mass of the cluster,  $\delta \langle n \rangle$  and  $\delta \langle V \rangle$  as changes of the average number density  $n$  and average velocity  $V$  of the bodies,  $\delta(\sigma_V)$  as the change of dispersion of the velocities of bodies, and  $\delta_k$  as the change of the average ratio of radial velocity ( $V_r$ ) to tangential velocity ( $V_t$ ). The changes of all these values are defined by formulae like formula (4).

Table III shows the time  $t_c$  of closest approach of the quasar and the cluster. This table also presents the final relative populations  $n_1, n_2, n_3, n_4$  and the masses  $m_1, m_2, m_3, m_4$  of the following 'subsystems':

1)  $n_1, m_1$  are the relative number and total mass of escapers from the full system of quasar and cluster (the subsystem 'total escapers');

2)  $n_2, m_2$  are the corresponding values for bodies belonging only to the cluster (the subsystem 'non-captured');

3)  $n_3, m_3$  are the corresponding values for bodies belonging simultaneously to the cluster and to the quasar (the subsystem 'common members');

4)  $n_4, m_4$  are the corresponding values for bodies belonging only to the quasar (the subsystem 'captured').

Table IV shows the final relative number and total masses  $(n_1, m_1), (n_2, m_2), (n_3, m_3), (n_4, m_4)$  for the bodies from the different mass groups  $N_{gr}$  inside the subsystems 1-4 for every model  $N_o$ .

Table V shows the changes in time  $t$  of the evolutionary parameters  $d, E, L, q, \langle R \rangle, R_m, \langle n \rangle, \langle V \rangle, \sigma_V, k$ . Table VI shows the changes in time  $t$  of the values  $d$  (the distance of the quasar from the centre of inertia of the cluster),  $R_m$  (the radius of a cluster), as well as the values of  $n_1, n_2, n_3, n_4$ , for models  $N_o$ . Figures 1-6 demonstrate the structure of systems at different times during the computations.

## 4. Analysis of the results

### 4.1 Weak and strong interactions of a quasar and a galaxy cluster

We consider ten models with various initial conditions. Model 1 has a zero-mass quasar: it is an isolated cluster. Model 2 has a small initial value of the virial coefficient  $q_0 = 0.25$ ; for this model we observe a weak influence of the quasar on the evolution of the

cluster. We also have weak interaction of the quasar and the galaxy cluster (the QGC, for brevity

) for large pericentric distance of approach (Model 8). Strong interaction in the QGC takes place in the case of larger values of the initial virial coefficient  $q_0$  ('hot' Models 3-5) and larger masses  $M$  of the quasar (Models 6, 7, 9, 10).

For Models 4-10 we find that the final relative motions of the QGC are slower than the initial ones. This is the result of the merger of systems; orbits of the components change, and the parabolic orbit transforms to an elliptic one with large eccentricity.

## **4.2 Changes of energy and angular momentum, and the expansion of the system.**

Tidal effects start when the quasar has its closest encounter point. After this, bridges and tails are formed. The central core becomes compact as the result of this approach.

The energy of the cluster with the bound members increases when it is near the pericentric point. This is because the quasar is always on one side of the cluster as a result of which the cluster continuously increases its energy. The mass loss (the process of escape) reaches a maximum during the close contact. The change in the energy remains nearly constant with small fluctuations after this time, in models in which disruption has not set in (Namboodiri & Kochhar 1990). In a weak encounter the variation of the energy with time is fairly smooth.

Angular momentum transfer takes place because of the presence of a gravitational quadrupole moment (Namboodiri & Kochhar 1991). As expected, the tidal force expands the cluster in the orbital plane and compresses it in the perpendicular direction, transforming the sphere into an ellipsoid. As a result, orbital angular momentum transforms into spin of the cluster. Table V show this result for various models.

The escaping particles carry away a large fraction of the internal spin of the cluster. As expected, the spins of the total system and of the bound part are aligned, within statistical fluctuations, with the direction of the initial orbital angular momentum of the pair.

## **4.3 Influence of the initial virial coefficient $q_0$ of a cluster and of the mass of a quasar**

We observe that the energy of the cluster increases with the virial coefficient  $q_0$ , and the energy becomes positive in the extreme case where  $q_0 = 0.9$ . In this case, a cluster disrupts quickly and most of the particles are drawn to the quasar. Only 25-30% of the

bodies remain with the cluster at time  $t_f$ . About 50% of the bodies are bound to the quasar. Also we observe a positive value of the energy of the cluster after collision, in the models with large mass  $M$  of the quasar (Models 6, 7 with  $M=5$ , as well as the Models 9, 10 with  $M=10$ ). We also find fluctuations in the energy of a cluster due to the intensive process of formation of close binaries and multiples.

With increasing  $q_0$  we have also a significant increase of angular momentum of the cluster, as well as of the mean ratio  $k$  of radial velocities to tangential ones, and of the radii  $\langle R \rangle$  and  $R_m$  of the cluster. Therefore, the expansion of the cluster and the anisotropy of the velocities inside it are more noticeable when  $q_0$  is large. The dispersion of velocities of the bodies in the cluster decreases with an increase of  $q_0$ . These values change very quickly and strongly in the case of large quasar mass. The virial coefficient  $q$  shows fluctuations: for small  $q_0$ ,  $q$  increases with time; for large  $q_0$  values of  $q$  initially fluctuate strongly and after sometime reach the value  $q = 0.5$ , i.e. the total system reaches the state of equilibrium (Models 1, 2, 3, 4, 8). For Models 5, 6, 7, 9, 10 the final virial coefficient  $q > 1$ ; in this case we have disruption of the cluster and capture of most of the bodies by the quasar. There are cases of full merger of the cluster with the quasar.

For all models except Model 2 both  $\langle R \rangle$  (the mean radius of a cluster without escapers) and  $R_m$  (the radius of the total system together with escapers) increase almost monotonically with time. For Model 2 we have initially a decrease in  $\langle R \rangle$ , indicating a collapse of the cluster. Later on this value increases; the value of  $R_m$  increases monotonically for this model. For larger  $q_0$  the expansion of the cluster is greater. For large masses  $M=5$  and 10 of the quasar, the effect of expansion of the cluster is less, especially for  $R_m$ . Model 5 with the largest  $q_0$  has the maximum expansion. For retrograde motion the expansion of the cluster is larger than for prograde motion of the bodies in the QGC.

The number density  $\langle n \rangle$  of galaxies is maximum for Models 6, 9, 10, with  $M = 5$  and 10. The density  $\langle n \rangle$  is minimum for Models 1 (no quasar) and 5, where we have a considerable expansion, many escapers, and the lowest density in the halo. For models with  $M = 5$  and 10 the final products have large number density; they are more compact objects, with high density and small radii.

The mean velocity of the galaxies initially increases and reaches a maximum at the time of closest approach. Later on mean velocities of the bodies belonging to the system decrease. The dispersion of velocities initially increases and reaches a maximum at the time  $t_c$  of closest approach of the QGC. After this, the dispersion decreases slightly, almost monotonically but with some fluctuations. At the final time  $t_f$ , a maximum of velocity

dispersion takes place for the models with the largest quasars ( $M=5$  and  $10$ ); the minimum of the dispersion is for Model 5. For the last model, we have very many escapers before  $t_f$ . The escapers carry away a large amount of kinetic energy from the cluster.

For the models with large  $q_0$ , the final motions of the galaxies inside the cluster are more radial, and the anisotropy of the velocities is larger. This effect corresponds to large expansion of the cluster. It is practically independent of the mass of the quasar; for retrograde motions of the QGC this effect is larger.

All of the values quoted above change very quickly during the closest approach of the quasar with the cluster; after this time, changes of these evolutionary parameters are almost monotonic with time.

#### 4.4 Final structures of the systems

Figures 1-6 demonstrate the structure of the final product of the collision of a quasar with a galaxy cluster. Fig. 1 for Model 1 with  $M = 0$  (no quasar) shows that the final structure has a central concentration of the high-mass bodies with multiples in the core. Similar structure is seen in Model 8. In these cases we observe a small effect of the perturbation of the quasar on the cluster.

For Models 3 and 4 (Fig. 2, 3) we have the capture of the cluster by the quasar, and the final configuration shows the cluster with the quasar inside close to its centre. For Model 5 (Fig. 4a, b) the quasar is exactly in the centre of total system. In this case, the final product has many observed characteristics of central cD-galaxies (see Introduction). Fig. 4a shows the structure of the system in the plane XY, which is the plane of the orbit of the QGC pair; Fig. 4b shows the same in the perpendicular plane XZ. In these two planes the structure of the total system is more or less similar. Figs 5, 6 show the structure of the final products in Models 6 and 9 with large mass ( $M=5$  and  $10$ ) for the quasar; for both models  $q_0=0.5$ . In these cases the structure of the system has the characteristics of observed gravitational lenses. The numerous faint dwarf galaxies form long arcs. In Model 6 with mass  $M=5$  of the quasar, the quasar is inside this arc. In Model 9 with  $M=10$ , the quasar is surrounded by these dwarf galaxies and lies at the center of curvature of the arc.

#### 4.5 Population of the ‘subsystems’ of the merger product

At the end of the computations we have four groups of particles: 1) escapers; 2) particles belonging only to the cluster; 3) common members belonging to the total QGC system; 4) particles belonging only to the quasar system. The particles of group 1 escape

from the total system and they have positive individual total energies with respect to the centre of mass of the cluster. For Model 1 with the zero-mass quasar, only light bodies escape from the system. For Models 2, 8 with weak interactions, galaxies with intermediate masses can escape from the system. In the final state of the total system the bodies with large masses usually belong to the cluster. As a rule, the quasar captures the light bodies. In cases of strong interaction of the quasar and the cluster (Models 3-7, 9, 10), galaxies with different masses escape from the total system (25-30%); sometimes escapers can carry away a significant part of the mass of the cluster. Bodies with any masses can also be common members of the final total system, as well as belonging only to the quasar. In the central part of the total system, there is an intense process of formation and disruption of multiples containing a quasar. For models with strong interaction within the QGC, we observe only about 15-30% of escapers. The other bodies belong to the total system; 10-25% of particles are drawn to the quasar. For models with weak interaction, the escape rate is in the range of 5-15% of the bodies, 5-10% of them belonging only to the quasar; 70-95% of the galaxies become common members of the total QGC system. With increasing  $q_0$  the number of escapers of various masses increases. There is no significant dependence on the mass  $M$  of the quasar. The number of common members decreases with increasing  $q_0$ . For large  $M$  the probability of capture of the high-mass bodies by the quasar is greater.

For all models (except Model 1), before the moment  $t_c$  of closest approach of the QGC there is a slight variation in the number  $n_1$  of bodies from Group 1 belonging only to the cluster. At time  $t_c$ , a drastic change takes place in this number. For models with weak interaction, the number  $n_2$  of the bodies belonging only to the cluster decreases almost monotonically. For other models with strong interaction,  $n_2$  decreases suddenly and becomes zero. Corresponding jumps of the number  $n_3$  of common members of the total system are also observed. Later these values  $n_2$  and  $n_3$  change slightly, with small fluctuations. The value  $n_4$  of the number of the bodies belonging only to the quasar's system changes similarly. Jumps of the values  $n_2$ ,  $n_3$ , and  $n_4$  are practically the same for all models except Model 1. With an increase of  $q_0$ , and of the mass of the quasar, the number and masses of escapers and galaxies captured by the quasar increase. There is a strong correlation between the values  $n_1$  and  $m_1$ ,  $n_2$  and  $m_2$ ,  $n_3$  and  $m_3$ ,  $n_4$  and  $m_4$ .

## 4.6 Multiples inside the full quasar-cluster system

For certain models, we observe final binaries or triples inside the full QGC system.

Sometimes these multiples contain a quasar, at other times they are formed by heavy bodies. Tables VII a, b show the data for isolated binaries and for binaries in isolated triples. These tables present the following values:  $t_f$  is the final time of evolution;  $m_1$  and  $m_2$  are the masses of the components of binaries;  $a$  and  $e$  are the semi-major axes and eccentricities of the binaries;  $r$  is the distance of a binary from the centre of mass of the full system. The last two columns show the number of binaries and triples which are formed and disrupted as the collision proceeds.

We can see that the process of formation and disruption of multiples is very intense in the central part of the QGC system. For Model 2 with the smallest  $q_0$ , we obtain a final quartet. One of the components of this multiple is the quasar.

## 5. Conclusion

We have examined tidal effects of the close approach of a quasar to a galaxy cluster. The quasar is a point-mass body ; the galaxy cluster is a spherical 250-body system with a spectrum of masses for the galaxies. We study collisions of these objects and consider a wide range of initial conditions for their initial parabolic approach.

We show that for small pericentric distances, large quasar mass, and large values for the initial virial coefficient  $q_0$  (kinetic energy over potential energy) of the cluster, collisions of the objects result in their merger. In general, about 30% of particles escape from the full system, and other particles are captured by the quasar. For the model with the largest initial virial coefficient  $q_0 = 0.90$ , the structure of the final remnant has many properties of cD-galaxies. For quasars with large masses, we obtain remnants with properties of gravitational lenses: a quasar surrounded by numerous light galaxies. These galaxies form long arcs with a large curvature. In the final stage of all models, quasars form binaries with faint galaxies.

During the course of the evolution of the full system, we find the formation of multiples containing a quasar and faint galaxies. These multiples have negative total energy. During strong close interactions of a few galaxies, multiples form and disrupt quickly inside the systems. We also obtain many close temporary and final multiples with high-mass components inside the clusters, at various distances from their centres.

## ACKNOWLEDGMENTS

We thank S. J. Aarseth for kindly sending us his NBODY2 code.

## References

- Barnes, J. E. , Hernquist, L. E. , 1992, *Ann. Rev. Astron. Astrophys.* 30, 705.
- Blandford, R. D. , Narayan, R. , 1992. *Ann. Rev. Astron. Astrophys.* 30, 311.
- French, H. B. , Gunn, J. E. , 1983. *Astrophys. J.* 269, 29.
- Heckman, T. M. , Bothun, C. D. , Balick, B. , Smith, E. P. 1984. *Astron. J.* 89, 958.
- Hutchings, J. B. , Janson, T. , Neff, S. G. 1989. *Astrophys. J.* 342, 660.
- MacKenty, J. W. , Stockton, A. 1984, *Astrophys. J.* 283, 64.
- Matthews, T. A, Morgan, W. W. , Schmidt, M. , 1964, *Astrophys. J.* , 140, 35.
- Morgan, W. W. , Lesh, J. R. 1965. *Astrophys. J. Lett.* 202, L113.
- Namboodiri, P. M. S. , Kochhar, R. K. 1990, *Mon. Not. Roy. Astron. Soc.* 243, 276.
- Namboodiri, P. M. S. , Kochhar, R. K. 1991a, *Mon. Not. Roy. Astron. Soc.* 250, 541.
- Namboodiri, P. M. S. , Kochhar, R. K. 1991b, *Mon. Not. Roy. Astron. Soc.* 253, 683.
- Namboodiri, P. M. S. , Kochhar, R. K. 1993, *Mon. Not. Roy. Astron. Soc.* 261, 855.
- Sanders, D. B. , Soifer, B. T. , Neugebauer, G. 1990. See Wielen 1990, 459.
- Schechter, P. L. 1980. *Astron. J.* 85, 801.
- Smith, R. M. , Efstathiou, G. , Ellis, R. S. , Frenk, C. S. , Valentijn, E. A. 1985. *Mon. Not. Roy. Astron. Soc.* 216, 71.
- Stockton, A. 1978. *Astrophys. J.* 223, 747.
- Stockton, A. , Ridgway, S. S. 1991. *Astron. J.* 102, 488.
- Sulentic, J. W. , Keel, W. C. , Telesco, C. M. eds. 1990. *Paired and Interacting Galaxies.* NASA.
- Tonry, J. L. 1984. *Astrophys. J.* 279, 13.
- Tonry, J. L. 1985. *Astron. J.* 90, 2431.
- Tonry, J. L. 1987. In *structure and dynamics of Elliptical galaxies*, IAU Symp. No. 127, ed. T. de Zeeuw, Dordrecht; Reidel 89.
- Toomre, A. , Toomre, J. 1972. *Astrophys. J.* 178, 623.
- Tremaine, S. 1990. See Wielen 1990, p394.
- Vader, J. P. , Da Costa, G. S. , Frogel, J. A. , Heisler, C. A. , Simon, M. 1987. *Astron. J.* 94, 847.
- White, R. A. 1978. *Ap. J.* 226, 591.
- White, S. D. M. 1983. In *Internal Kinematics and Dynamics of Galaxies*, ed. E. Athanassoula, 337, Dordrecht, Reidel.
- White, S. D. M. , Rees, M. J. 1978. *Mon. Not. Roy. Astron. Soc.* 183, 341.

Wielen. R. ed. 1990. Dynamics and Interactions of Galaxies. Berlin: Springer-Verlag.

TABLE I

The initial parameters of models

$N_o$	$q_0$	$M$	$\delta_F$	$p$	$d_0$	$t_f$	$N_o$	$q_0$	$M$	$\delta_F$	$p$	$d_0$	$t_f$	
1	0.50	0	-	-	-	10	6	0.50	5.0	1.25	3.0	6.0	10	
2	0.25	1.0	0.25	4.0	8.0	40	7	0.50	5.0	0.27	3.0	10.0	20	*
3	0.50	1.0	0.25	3.0	6.0	30	8	0.50	5.0	3.60	8.0	11.0	20	
4	0.75	1.0	0.25	1.5	3.0	20	9	0.50	10.0	2.50	3.0	6.0	10	
5	0.90	1.0	0.002	0.4	4.0	20	10	0.50	10.0	0.23	3.0	13.0	20	*

TABLE Ia

The groups of masses of the bodies in the cluster

N=250, M1=1.000

$N_{gr}$	$n$	$m$	$sum_m$
1	5	0.04	0.20
2	10	0.02	0.20
3	20	0.01	0.20
4	40	0.005	0.20
5	175	0.00114	0.20

TABLE II

The maximal relative changes of evolutionary parameters of clusters

$N_o$	$\delta_E$	$\delta_L$	$\delta_q$	$\delta \langle R \rangle$	$\delta(Rm)$	$\delta \langle n \rangle$	$\delta \langle V \rangle$	$\delta(\sigma_V)$	$\delta_k$
1	0.107	0	0.622	2.973	10.664	1.045	0.674	0.632	0.296
2	0.625	3.242	1.600	5.323	10.669	4.783	0.902	2.727	0.845
3	0.432	6.618	0.435	5.527	16.728	3.281	0.633	1.053	0.762
4	0.668	6.340	0.851	13.482	29.193	0.583	1.016	0.406	1.324
5	1.762	9.985	1.149	69.045	153.907	7.400	1.173	0.196	2.042
6	1.917	17.091	2.120	2.991	6.714	4.562	0.451	2.316	0.738
7	5.583	21.268	6.292	7.964	12.700	-	0.915	3.632	1.911
8	0.108	3.487	0.386	2.580	10.530	-	0.386	0.842	0.446
9	3.044	27.571	3.240	4.611	7.793	4.562	0.775	3.263	0.841
10	2.725	23.527	3.480	7.455	11.101	4.774	0.831	4.684	1.574

TABLE III

The final relative population and masses of subsystems

<i>number</i> $N_0$ <i>models</i>	<i>time</i> $t_c$ <i>cl.ap.</i>	<i>the</i> $n_1$ <i>esc</i>	<i>numbers</i> $n_2$ <i>non - capt</i>	<i>of</i> $n_3$ <i>comm</i>	<i>bodies</i> $n_4$ <i>capt</i>	<i>the</i> $m_1$ <i>esc</i>	<i>masses</i> $m_2$ <i>non - capt</i>	<i>of</i> $m_3$ <i>comm</i>	<i>bodies</i> $m_4$ <i>capt</i>
1	-	0.084	-	0.916	-	0.036	-	0.964	-
2	10	0.164	0.060	0.704	0.072	0.094	0.059	0.811	0.036
3	8	0.160	0	0.720	0.120	0.173	0	0.767	0.059
4	2	0.268	0	0.624	0.108	0.185	0	0.749	0.066
5	4	0.540	0	0.244	0.216	0.492	0	0.332	0.176
6	4	0.228	0	0.548	0.224	0.170	0	0.652	0.178
7	8	0.380	0	0.228	0.392	0.340	0	0.364	0.295
8	10	0.064	0.132	0.728	0.076	0.022	0.102	0.846	0.029
9	3	0.264	0	0.440	0.296	0.195	0	0.492	0.313
10	8	0.344	0	0.364	0.292	0.331	0	0.467	0.202

TABLE IV

Final relative number and total mass of unequal-mass bodies in subsystems

$N_{gr}$ groups	$n_1$ tot.	$m_1$ esc	$n_2$ non	$m_2$ capt	$n_3$ comm.	$m_3$ memb.	$n_4$ capt.	$m_4$ memb.
<i>model</i>	1							
1	0	0	-	-	0.020	0.200	-	-
2	0	0	-	-	0.040	0.200	-	-
3	0	0	-	-	0.080	0.200	-	-
4	0.012	0.015	-	-	0.148	0.185	-	-
5	0.072	0.021	-	-	0.628	0.179	-	-
<i>tot</i>	0.084	0.036	-	-	0.916	0.964	-	-
<i>model</i>	2							
1	0	0	0	0	0.020	0.200	0	0
2	0.004	0.020	0	0	0.036	0.180	0	0
3	0.004	0.010	0.012	0.030	0.064	0.160	0	0
4	0.020	0.025	0.016	0.020	0.108	0.135	0.016	0.020
5	0.136	0.039	0.032	0.009	0.476	0.136	0.056	0.016
<i>tot</i>	0.164	0.094	0.060	0.059	0.704	0.811	0.072	0.036
<i>model</i>	3							
1	0.004	0.040	0	0	0.016	0.160	0	0
2	0	0	0	0	0.040	0.200	0	0
3	0.028	0.070	0	0	0.048	0.120	0.004	0.010
4	0.028	0.035	0	0	0.116	0.145	0.016	0.020
5	0.100	0.028	0	0	0.500	0.142	0.100	0.030
<i>tot</i>	0.160	0.173	0	0	0.720	0.767	0.120	0.060
<i>model</i>	4							
1	0.004	0.040	0	0	0.016	0.160	0	0
2	0	0	0	0	0.036	0.180	0.004	0.020
3	0.016	0.040	0	0	0.064	0.160	0	0
4	0.036	0.045	0	0	0.108	0.135	0.016	0.020
5	0.212	0.060	0	0	0.400	0.114	0.088	0.026
<i>tot</i>	0.268	0.185	0	0	0.624	0.749	0.108	0.066
<i>model</i>	5							
1	0.008	0.080	0	0	0.012	0.120	0	0
2	0.012	0.060	0	0	0.016	0.080	0.012	0.060
3	0.052	0.130	0	0	0.016	0.040	0.012	0.030
4	0.092	0.115	0	0	0.036	0.045	0.032	0.040
5	0.376	0.107	0	0	0.164	0.047	0.160	0.046
<i>tot</i>	0.540	0.492	0	0	0.244	0.332	0.216	0.176

TABLE IV

Final relative number and total mass of unequal-mass bodies in subsystems (continued)

$N_{gr}$ <i>groups</i>	$n_1$ <i>tot.</i>	$m_1$ <i>esc</i>	$n_2$ <i>non</i>	$m_2$ <i>capt</i>	$n_3$ <i>comm.</i>	$m_3$ <i>memb.</i>	$n_4$ <i>capt.</i>	$m_4$ <i>memb.</i>
<i>model</i>	6							
1	0.004	0.040	0	0	0.012	0.120	0.004	0.040
2	0	0	0	0	0.036	0.180	0.004	0.020
3	0.016	0.040	0	0	0.056	0.140	0.008	0.020
4	0.032	0.040	0	0	0.088	0.111	0.040	0.050
5	0.176	0.050	0	0	0.356	0.101	0.168	0.048
<i>tot</i>	0.228	0.170	0	0	0.548	0.652	0.224	0.178
<i>model</i>	7							
1	0.008	0.080	0	0	0.012	0.120	0	0
2	0.012	0.060	0	0	0.016	0.080	0.012	0.060
3	0.016	0.040	0	0	0.024	0.060	0.040	0.100
4	0.064	0.080	0	0	0.056	0.070	0.040	0.050
5	0.280	0.080	0	0	0.120	0.034	0.300	0.085
<i>tot</i>	0.380	0.340	0	0	0.228	0.364	0.392	0.295
<i>model</i>	8							
1	0	0	0	0	0.020	0.200	0	0
2	0	0	0.004	0.020	0.036	0.180	0	0
3	0	0	0.012	0.030	0.068	0.170	0	0
4	0.004	0.005	0.020	0.025	0.128	0.160	0.008	0.010
5	0.060	0.017	0.096	0.027	0.476	0.136	0.068	0.019
<i>tot</i>	0.064	0.022	0.132	0.102	0.728	0.846	0.076	0.029
<i>model</i>	9							
1	0	0	0	0	0.008	0.080	0.012	0.120
2	0.008	0.040	0	0	0.024	0.120	0.008	0.040
3	0.016	0.040	0	0	0.048	0.120	0.016	0.040
4	0.048	0.060	0	0	0.072	0.090	0.040	0.050
5	0.192	0.055	0	0	0.288	0.082	0.220	0.063
<i>tot</i>	0.264	0.195	0	0	0.440	0.492	0.296	0.313
<i>model</i>	10							
1	0.008	0.080	0	0	0.012	0.120	0	0
2	0.008	0.040	0	0	0.028	0.140	0.004	0.020
3	0.032	0.080	0	0	0.024	0.060	0.024	0.060
4	0.052	0.060	0	0	0.064	0.080	0.044	0.060
5	0.244	0.070	0	0	0.236	0.067	0.220	0.062
<i>tot</i>	0.344	0.330	0	0	0.364	0.467	0.292	0.202

TABLE V

The current evolutionary parameters of clusters

$t$	$d$	$E$	$L$	$q$	$\langle R \rangle$	$R_m$	$\langle n \rangle$	$\langle V \rangle$	$\sigma_V$	$k$
<i>model</i>	1									
0	-	-0.250	0.112	0.50	1.12	2.17	3.1	0.71	0.19	0.71
1	-	-0.264	0.112	0.60	1.25	4.01	4.5	0.77	0.31	0.77
2	-	-0.255	0.112	0.47	1.78	5.48	2.8	0.63	0.26	0.75
3	-	-0.252	0.112	0.41	2.23	8.07	3.0	0.56	0.26	0.78
4	-	-0.260	0.112	0.44	2.59	10.67	3.1	0.54	0.26	0.80
5	-	-0.258	0.112	0.50	2.90	13.19	2.7	0.54	0.31	0.78
6	-	-0.264	0.112	0.50	3.18	15.67	2.4	0.53	0.27	0.86
7	-	-0.255	0.112	0.44	3.45	18.11	2.5	0.52	0.27	0.88
8	-	-0.280	0.112	0.46	3.75	20.53	2.6	0.52	0.29	0.92
9	-	-0.280	0.112	0.37	4.16	22.93	2.2	0.46	0.25	0.87
10	-	-0.273	0.112	0.43	4.45	25.31	2.5	0.47	0.28	0.86
<i>model</i>	2									
0	8.00	-0.250	0.097	0.25	1.67	3.26	2.3	0.41	0.11	0.71
2	7.00	-0.252	0.095	0.51	1.48	3.88	11.2	0.61	0.28	0.76
4	6.00	-0.251	0.094	0.59	1.27	4.42	13.3	0.75	0.34	0.71
6	5.13	-0.250	0.091	0.56	1.33	4.69	10.9	0.78	0.34	0.77
8	4.41	-0.244	0.104	0.51	1.67	5.25	9.4	0.70	0.32	0.79
10	4.02	-0.243	0.161	0.52	2.03	6.81	7.9	0.64	0.29	0.85
12	4.11	-0.244	0.172	0.51	2.41	9.02	6.7	0.59	0.29	0.87
14	4.54	-0.233	0.211	0.56	2.75	10.85	6.3	0.60	0.31	0.86
16	5.23	-0.237	0.249	0.56	3.10	12.39	6.1	0.61	0.34	0.84
18	6.04	-0.254	0.282	0.61	3.52	14.42	5.2	0.59	0.38	0.93
20	6.90	-0.324	0.292	0.65	3.81	16.82	4.6	0.59	0.41	1.01
22	7.80	-0.622	0.328	0.42	4.21	19.14	3.6	0.59	0.34	1.06
24	8.60	-0.305	0.318	0.46	4.65	21.41	3.6	0.54	0.27	1.20
26	9.50	-0.347	0.315	0.50	5.11	23.63	4.7	0.53	0.29	1.04
28	10.30	-0.464	0.330	0.40	5.61	25.79	3.7	0.51	0.29	1.11
30	11.20	-0.283	0.313	0.51	6.08	27.92	3.8	0.49	0.28	1.16
32	12.00	-0.328	0.386	0.34	6.50	30.01	3.7	0.45	0.24	1.25
34	12.70	-0.240	0.345	0.46	6.81	32.09	4.8	0.46	0.25	1.17
36	13.50	-0.256	0.327	0.40	7.24	34.13	4.7	0.47	0.28	1.24
38	14.30	-0.319	0.350	0.43	7.65	36.15	4.8	0.46	0.27	1.27
40	15.00	-0.234	0.324	0.57	8.03	38.14	4.1	0.48	0.30	1.31

TABLE V

The current evolutionary parameters of clusters (continuation 1)

$t$	$d$	$E$	$L$	$q$	$\langle R \rangle$	$R_m$	$\langle n \rangle$	$\langle V \rangle$	$\sigma_V$	$k$
<i>model</i>	3									
0	6.00	-0.250	0.112	0.50	1.12	2.17	3.2	0.71	0.19	0.71
2	4.90	-0.251	0.110	0.62	1.13	3.47	13.7	0.80	0.34	0.63
4	3.80	-0.251	0.102	0.46	1.53	4.48	8.2	0.64	0.25	0.77
6	3.10	-0.222	0.194	0.53	1.87	6.60	8.4	0.65	0.37	0.69
8	3.00	-0.197	0.294	0.62	2.23	9.07	7.8	0.71	0.39	0.81
10	3.50	-0.308	0.437	0.52	2.70	11.49	6.7	0.69	0.39	0.90
12	4.20	-0.203	0.448	0.60	3.19	13.75	5.6	0.66	0.31	0.98
14	5.00	-0.209	0.498	0.52	3.74	15.88	5.0	0.60	0.29	1.03
16	5.80	-0.197	0.518	0.48	4.25	18.55	5.2	0.54	0.27	1.05
18	6.50	-0.175	0.567	0.60	4.73	21.49	5.9	0.54	0.29	1.05
20	7.20	-0.180	0.618	0.53	5.14	24.38	5.5	0.55	0.28	1.01
22	7.90	-0.187	0.612	0.49	5.56	27.25	5.9	0.52	0.27	1.08
24	8.50	-0.196	0.583	0.66	5.96	30.09	6.3	0.55	0.33	0.92
26	9.00	-0.178	0.651	0.60	6.42	32.89	4.2	0.51	0.28	1.11
28	9.60	-0.182	0.683	0.53	6.87	35.69	4.8	0.49	0.28	1.04
30	10.00	-0.179	0.777	0.60	7.31	38.47	5.0	0.50	0.31	1.04
<i>model</i>	4									
0	3.00	-0.250	0.097	0.75	0.56	1.09	7.6	1.23	0.33	0.71
2	1.57	-0.083	0.280	0.87	1.29	3.20	7.3	0.88	0.45	0.87
4	2.07	-0.141	0.417	0.75	2.00	5.90	6.1	0.83	0.42	1.06
6	3.22	-0.228	0.431	0.66	2.69	9.29	7.1	0.83	0.38	1.21
8	4.30	-0.148	0.413	0.77	3.51	12.73	7.1	0.84	0.41	1.30
10	5.16	-0.090	0.566	0.81	4.38	16.17	5.7	0.74	0.34	1.36
12	5.82	-0.165	0.675	0.72	5.24	19.56	5.7	0.69	0.38	1.39
14	6.49	-0.233	0.689	0.58	6.01	22.91	4.9	0.64	0.33	1.51
16	7.14	-0.204	0.712	0.65	6.73	26.26	5.8	0.64	0.35	1.41
18	7.78	-0.244	0.696	0.47	7.43	29.58	4.8	0.61	0.32	1.65
20	8.40	-0.164	0.661	0.63	8.11	32.91	5.8	0.62	0.36	1.35

TABLE V

The current evolutionary parameters of clusters (continuation 2)

$t$	$d$	$E$	$L$	$q$	$\langle R \rangle$	$R_m$	$\langle n \rangle$	$\langle V \rangle$	$\sigma_V$	$k$
<i>model</i>	5									
0	4.00	-0.250	0.067	0.90	0.22	0.43	21.00	2.13	0.57	0.71
2	1.95	-0.261	0.074	0.74	1.77	6.32	4.8	1.10	0.54	1.57
4	0.37	0.229	0.710	1.34	3.39	13.25	2.9	1.30	0.51	1.57
6	0.85	0.082	0.608	1.11	5.14	20.03	2.8	1.08	0.56	2.16
8	0.85	0.084	0.633	1.14	6.69	26.60	2.6	1.04	0.55	2.06
10	0.82	0.262	0.668	1.59	8.16	33.24	2.7	1.09	0.58	1.84
12	0.96	0.097	0.658	1.20	9.68	40.03	2.5	1.02	0.56	2.10
14	1.09	-0.344	0.679	0.69	11.19	46.67	2.6	0.98	0.55	2.00
16	1.38	0.170	0.655	1.35	12.62	53.33	2.5	1.01	0.58	1.91
18	1.56	0.102	0.736	1.17	14.00	60.08	2.7	1.00	0.57	1.86
20	1.81	-0.164	0.630	0.84	15.41	66.61	2.6	1.02	0.61	1.85
<i>model</i>	6									
0	6.00	-0.250	0.112	0.50	1.12	2.17	3.2	0.71	0.19	0.71
1	5.01	-0.301	0.107	0.62	1.08	2.79	12.3	0.80	0.34	0.65
2	4.06	-0.242	0.099	0.61	1.14	3.36	16.1	0.83	0.36	0.65
3	3.28	-0.106	0.248	0.80	1.36	4.30	17.4	0.85	0.51	0.70
4	2.85	0.276	0.930	1.56	1.68	5.91	17.8	0.98	0.63	0.75
5	2.96	0.239	1.386	1.43	2.07	7.96	17.0	1.03	0.60	0.77
6	3.48	0.172	1.517	1.41	2.49	9.98	17.0	0.95	0.52	0.85
7	4.18	0.124	1.614	1.32	2.92	11.84	16.3	0.91	0.48	0.93
8	4.93	0.092	1.698	1.25	3.39	13.57	16.2	0.87	0.45	1.04
9	5.69	-0.008	1.767	0.98	3.84	15.19	15.7	0.85	0.44	1.06
10	6.44	0.062	1.791	1.21	4.31	16.74	15.5	0.81	0.43	1.13
<i>model</i>	7									
0	11.00	-0.250	0.112	0.50	1.12	2.17	-	0.71	0.19	0.71
2	8.99	-0.250	0.112	0.61	1.13	3.49	-	0.80	0.34	0.66
4	6.80	-0.252	0.113	0.48	1.49	4.56	-	0.68	0.26	0.74
6	4.33	-0.228	0.115	0.54	1.87	5.60	-	0.72	0.34	0.86
8	1.75	1.155	1.579	3.50	2.32	7.15	-	1.30	0.88	0.56
10	1.85	0.482	1.854	1.85	3.33	9.51	-	1.36	0.64	1.01
12	3.54	0.262	1.790	1.78	4.76	12.46	-	1.08	0.50	1.24
14	5.06	0.169	1.634	1.52	6.13	16.38	-	0.95	0.41	1.50
16	6.34	0.186	1.795	1.78	7.48	20.94	-	0.88	0.44	1.50
18	7.48	0.134	1.787	1.52	8.78	25.40	-	0.82	0.37	1.63
20	8.44	0.236	2.494	1.96	10.04	29.73	-	0.81	0.43	1.48

TABLE V

The current evolutionary parameters of clusters (continuation 3)

$t$	$d$	$E$	$L$	$q$	$\langle R \rangle$	$R_m$	$\langle n \rangle$	$\langle V \rangle$	$\sigma_V$	$k$
<i>model</i>	8									
0	11.00	-0.250	0.112	0.50	1.12	2.17	-	0.71	0.19	0.71
2	9.96	-0.250	0.114	0.61	1.13	3.50	-	0.79	0.31	0.65
4	9.07	-0.251	0.116	0.47	1.49	4.65	-	0.66	0.24	0.72
6	8.41	-0.249	0.118	0.48	1.83	5.63	-	0.61	0.28	0.92
8	8.04	-0.249	0.115	0.44	2.12	6.55	-	0.57	0.25	0.87
10	8.02	-0.224	0.078	0.51	2.42	8.62	-	0.59	0.34	0.94
12	8.35	-0.227	0.141	0.45	2.75	12.53	-	0.56	0.32	0.86
14	8.98	-0.279	0.212	0.51	3.05	15.87	-	0.60	0.35	0.80
16	9.82	-0.229	0.269	0.49	3.33	19.05	-	0.61	0.33	0.82
18	10.80	-0.238	0.309	0.50	3.64	22.09	-	0.62	0.34	0.82
20	11.86	-0.236	0.350	0.53	4.01	25.02	-	0.59	0.32	0.89
<i>model</i>	9									
0	6.00	-0.250	0.112	0.50	1.12	2.17	3.2	0.71	0.19	0.71
1	4.66	-0.246	0.101	0.62	1.08	2.76	11.9	0.80	0.33	0.63
2	3.48	-0.093	0.146	0.84	1.18	4.47	16.5	0.93	0.63	0.71
3	2.87	0.353	0.929	1.69	1.57	6.02	17.8	1.15	0.81	0.75
4	3.21	0.511	1.749	2.12	2.12	8.25	17.7	1.26	0.75	0.83
5	4.13	0.401	2.089	1.89	2.76	10.44	17.4	1.17	0.66	0.96
6	5.21	0.318	2.308	1.79	3.42	12.42	17.0	1.11	0.59	1.05
7	6.29	0.283	2.504	1.78	4.06	14.23	16.6	1.08	0.57	1.08
8	7.33	0.261	2.723	1.62	4.74	15.93	16.5	1.05	0.58	1.15
9	8.32	0.253	2.947	1.84	5.40	17.54	16.3	1.01	0.55	1.16
10	9.28	0.251	3.200	1.76	6.06	19.08	16.3	1.01	0.54	1.16
<i>model</i>	10									
0	13.00	-0.250	0.112	0.50	1.12	2.17	3.1	0.71	0.19	0.71
2	10.64	-0.276	0.112	0.63	1.13	3.48	16.2	0.81	0.34	0.66
4	8.12	-0.252	0.114	0.54	1.50	4.56	17.8	0.69	0.26	0.72
6	5.44	-0.223	0.130	0.54	1.88	5.42	17.9	0.66	0.28	0.79
8	3.08	0.472	1.000	2.11	2.38	6.69	17.2	1.24	1.08	0.54
10	3.22	0.476	2.344	2.24	3.32	10.57	16.8	1.30	0.71	0.83
12	5.22	0.271	2.457	1.85	4.61	14.27	16.5	1.10	0.56	1.07
14	7.31	0.097	2.530	1.22	5.91	17.47	16.5	1.00	0.51	1.20
16	9.25	0.134	2.721	1.38	7.19	20.38	16.6	0.94	0.53	1.17
18	11.08	0.089	2.747	1.31	8.35	23.12	17.2	0.86	0.44	1.31
20	12.79	0.083	2.746	1.27	9.47	26.26	17.7	0.83	0.47	1.39

TABLE VI

The current relative population of subsystems

<i>t</i>	<i>d</i>	<i>R<sub>m</sub></i>	<i>n<sub>1</sub></i>	<i>n<sub>2</sub></i>	<i>n<sub>3</sub></i>	<i>n<sub>4</sub></i>	<i>t</i>	<i>d</i>	<i>R<sub>m</sub></i>	<i>n<sub>1</sub></i>	<i>n<sub>2</sub></i>	<i>n<sub>3</sub></i>	<i>n<sub>4</sub></i>
-	<i>dist</i>	<i>rad</i>	<i>esc</i>	<i>n.cap</i>	<i>comm</i>	<i>cap</i>	-	<i>dist</i>	<i>rad</i>	<i>esc</i>	<i>n.cap</i>	<i>comm</i>	<i>cap</i>
-	<i>model</i>	1											
0	-	2.17	0.004	-	0.996	-							
1	-	4.01	0.028	-	0.972	-	6	-	15.67	0.064	-	0.936	-
2	-	5.48	0.032	-	0.968	-	7	-	18.11	0.068	-	0.932	-
3	-	8.07	0.044	-	0.956	-	8	-	20.53	0.080	-	0.920	-
4	-	10.67	0.052	-	0.948	-	9	-	22.93	0.084	-	0.916	-
5	-	13.19	0.060	-	0.940	-	10	-	25.31	0.084	-	0.916	-
-	<i>model</i>	2											
0	8.00	3.26	0	1.000	0	0							
2	7.00	3.88	0	1.000	0	0	22	7.8	19.14	0.096	0.124	0.700	0.080
4	6.00	4.42	0.008	0.988	0	0.004	24	8.6	21.41	0.108	0.148	0.676	0.068
6	5.13	4.69	0.008	0.976	0	0.016	26	9.5	23.63	0.120	0.136	0.664	0.080
8	4.41	5.25	0.028	0.240	0.704	0.028	28	10.3	25.79	0.128	0.128	0.664	0.080
10	4.02	6.81	0.040	0.296	0.636	0.028	30	11.2	27.92	0.124	0.092	0.704	0.080
12	4.11	9.02	0.052	0.300	0.608	0.040	32	12.1	30.01	0.132	0.068	0.724	0.076
14	4.54	10.85	0.056	0.220	0.664	0.060	34	12.7	32.09	0.148	0.088	0.696	0.068
16	5.23	12.34	0.064	0.188	0.676	0.072	36	13.5	34.13	0.152	0.096	0.684	0.068
18	6.04	14.42	0.072	0.168	0.688	0.072	38	14.3	36.15	0.148	0.072	0.700	0.080
20	6.90	16.82	0.084	0.136	0.704	0.076	40	15.0	38.14	0.164	0.060	0.704	0.072
-	<i>model</i>	3											
0	6.0	2.17	0.004	0.996	0	0	16	5.8	18.55	0.096	0.044	0.732	0.128
2	4.9	3.47	0.008	0.988	0	0.004	18	6.5	21.49	0.112	0.008	0.760	0.120
4	3.8	4.48	0.036	0.304	0.648	0.012	20	7.2	24.38	0.116	0	0.764	0.120
6	3.1	6.60	0.060	0.300	0.612	0.028	22	7.9	27.25	0.124	0	0.756	0.120
8	3.0	9.07	0.068	0.276	0.580	0.076	24	8.5	30.09	0.128	0	0.752	0.120
10	3.5	11.49	0.084	0.200	0.636	0.080	26	9.0	32.89	0.136	0	0.736	0.128
12	4.2	13.75	0.100	0.160	0.656	0.084	28	9.6	35.69	0.144	0	0.728	0.128
14	5.0	15.88	0.100	0.076	0.712	0.112	30	10.0	38.47	0.160	0	0.720	0.120
-	<i>model</i>	4											
0	3.00	1.09	0.080	0.912	0	0.008							
2	1.57	3.20	0.148	0.268	0.536	0.048	12	5.82	19.56	0.248	0	0.612	0.140
4	2.07	5.90	0.176	0.096	0.624	0.104	14	6.49	22.91	0.260	0	0.616	0.124
6	3.22	9.29	0.204	0.048	0.632	0.116	16	7.14	26.26	0.256	0	0.620	0.124
8	4.30	12.73	0.244	0	0.636	0.120	18	7.78	29.58	0.260	0	0.628	0.112
10	5.16	16.17	0.248	0	0.612	0.140	20	8.40	32.91	0.268	0	0.624	0.108

TABLE VI

The current relative population of subsystems (continuation 1)

<i>t</i>	<i>d</i>	<i>R<sub>m</sub></i>	<i>n<sub>1</sub></i>	<i>n<sub>2</sub></i>	<i>n<sub>3</sub></i>	<i>n<sub>4</sub></i>	<i>t</i>	<i>d</i>	<i>R<sub>m</sub></i>	<i>n<sub>1</sub></i>	<i>n<sub>2</sub></i>	<i>n<sub>3</sub></i>	<i>n<sub>4</sub></i>
—	<i>dist</i>	<i>rad</i>	<i>esc</i>	<i>n.cap</i>	<i>comm</i>	<i>cap</i>	—	<i>dist</i>	<i>rad</i>	<i>esc</i>	<i>n.cap</i>	<i>comm</i>	<i>cap</i>
—	<i>model</i>	5											
0	4.00	0.43	0.168	0.796	0	0.036							
2	1.95	6.32	0.328	0.160	0.452	0.060	12	0.96	40.03	0.516	0	0.240	0.244
4	0.37	13.25	0.452	0	0.232	0.316	14	1.09	46.67	0.508	0	0.280	0.212
6	0.85	20.03	0.476	0	0.304	0.220	16	1.38	53.33	0.524	0	0.272	0.204
8	0.85	26.60	0.484	0	0.292	0.224	18	1.56	60.08	0.516	0	0.248	0.236
10	0.82	33.24	0.500	0	0.244	0.256	20	1.81	66.61	0.540	0	0.244	0.216
—	<i>model</i>	6											
0	6.00	2.17	0.004	0.996	0	0							
1	5.01	2.79	0	1.000	0	0	6	3.48	9.98	0.172	0	0.608	0.220
2	4.06	3.36	0.012	0.968	0	0.020	7	4.18	11.84	0.180	0	0.584	0.236
3	3.28	4.30	0.044	0.308	0.584	0.064	8	4.93	13.57	0.204	0	0.580	0.216
4	2.85	5.91	0.112	0.176	0.580	0.132	9	5.69	15.19	0.220	0	0.556	0.224
5	2.96	7.96	0.144	0.052	0.620	0.184	10	6.44	16.74	0.228	0	0.548	0.224
—	<i>model</i>	7											
0	11.00	2.17	0.004	0.996	0	0							
2	8.99	3.49	0.012	0.980	0	0.008	12	3.54	12.46	0.352	0	0.296	0.352
4	6.80	4.56	0.028	0.952	0	0.020	14	5.06	16.38	0.376	0	0.292	0.332
6	4.33	5.60	0.040	0.272	0.652	0.036	16	6.34	20.94	0.380	0	0.272	0.348
8	1.75	7.15	0.280	0	0.452	0.268	18	7.48	25.40	0.384	0	0.256	0.360
10	1.85	9.51	0.360	0	0.284	0.356	20	8.44	29.73	0.380	0	0.228	0.392

TABLE VI

The current relative population of subsystems (continuation 2)

$t$	$d$	$R_m$	$n_1$	$n_2$	$n_3$	$n_4$	$t$	$d$	$R_m$	$n_1$	$n_2$	$n_3$	$n_4$
—	<i>dist</i>	<i>rad</i>	<i>esc</i>	<i>n.cap</i>	<i>comm</i>	<i>cap</i>	—	<i>dist</i>	<i>rad</i>	<i>esc</i>	<i>n.cap</i>	<i>comm</i>	<i>cap</i>
—	<i>model</i>	8											
0	11.00	2.17	0.004	0.996	0	0							
2	9.96	3.50	0.008	0.988	0	0.004	12	8.35	12.53	0.044	0.220	0.684	0.052
4	9.07	4.65	0.008	0.976	0	0.016	14	8.98	15.87	0.044	0.224	0.672	0.060
6	8.41	5.63	0.016	0.972	0	0.012	16	9.82	19.05	0.052	0.212	0.668	0.068
8	8.04	6.55	0.016	0.952	0	0.032	18	10.80	22.09	0.052	0.200	0.672	0.076
10	8.02	8.62	0.036	0.216	0.704	0.044	20	11.86	25.02	0.064	0.132	0.728	0.076
—	<i>model</i>	9											
0	6.00	2.17	0.004	0.996	0	0							
1	4.66	2.76	0	0.992	0	0.008	6	5.21	12.42	0.240	0	0.508	0.252
2	3.48	4.47	0.056	0.256	0.612	0.076	7	6.29	14.23	0.256	0	0.489	0.256
3	2.87	6.02	0.160	0.080	0.572	0.188	8	7.33	15.93	0.269	0	0.476	0.256
4	3.21	8.25	0.212	0	0.548	0.240	9	8.32	17.54	0.256	0	0.472	0.272
5	4.13	10.44	0.232	0	0.512	0.256	10	9.28	19.08	0.264	0	0.440	0.296
—	<i>model</i>	10											
0	13.00	2.17	0.004	0.996	0	0							
2	10.64	3.48	0.008	0.988	0	0.004	12	5.22	14.27	0.336	0	0.368	0.296
4	8.12	4.56	0.012	0.968	0	0.020	14	7.31	17.47	0.328	0	0.376	0.296
6	5.44	5.42	0.052	0.236	0.660	0.052	16	9.25	20.38	0.336	0	0.364	0.300
8	3.08	6.69	0.192	0.028	0.584	0.196	18	11.08	23.12	0.340	0	0.372	0.288
10	3.22	10.55	0.340	0	0.368	0.292	20	12.79	26.26	0.344	0	0.364	0.292

TABLE VIIa  
Final multiple with quasar

$N_o$	$t_f$	$m_1$	$m_2$	$a$	$e$	$r$	$d$	$n_b$	$n_t$
2	40	1.000	0.005	0.610	0.816	6.52	15.00	4	5
2	40	1.000	0.001	0.348	0.814	7.40	15.00	4	5
2	40	1.000	0.001	1.018	0.703	7.13	15.00	4	5
3	30	1.000	0.001	0.524	0.951	4.24	10.00	6	2
4	20	1.000	0.001	0.117	0.840	3.98	8.40	4	4
5	20	1.000	0.010	0.082	0.305	0.86	1.81	5	2
6	10	5.000	0.001	0.544	0.519	0.75	6.44	3	0
9	10	10.000	0.001	1.266	0.411	2.35	9.28	2	3
10	20	10.000	0.001	0.926	0.424	1.23	11.92	3	1

TABLE VIIb  
Final multiple without quasar

$N_o$	$t_f$	$m_1$	$m_2$	$a$	$e$	$r$	$d$	$n_b$	$n_t$
1	10	0.04	0.04	0.005	0.471	0.11	-	16	0
2	40	0.04	0.04	0.017	0.373	1.08	15.00	21	0
2	40	0.04	0.04	0.008	0.377	1.08	15.00	21	0
3	30	0.04	0.04	0.008	0.647	5.27	10.00	12	0
4	20	0.04	0.04	0.006	0.633	5.56	8.40	12	0
5	20	0.04	0.04	0.003	0.303	0.97	1.81	23	0
6	10	0.04	0.02	0.007	0.358	8.60	6.44	11	0
9	10	0.04	0.04	0.012	0.966	10.68	9.28	9	0
10	20	0.04	0.02	0.004	0.798	12.35	12.79	24	0

## Captions

**Fig.1.** The structure of system for the model 1 (the isolated cluster;  $q_0=0.5, M=0$ ) at various times.

**Fig.2.** The structure of system for the model 3 ( $q_0=0.50, M=1$ ).

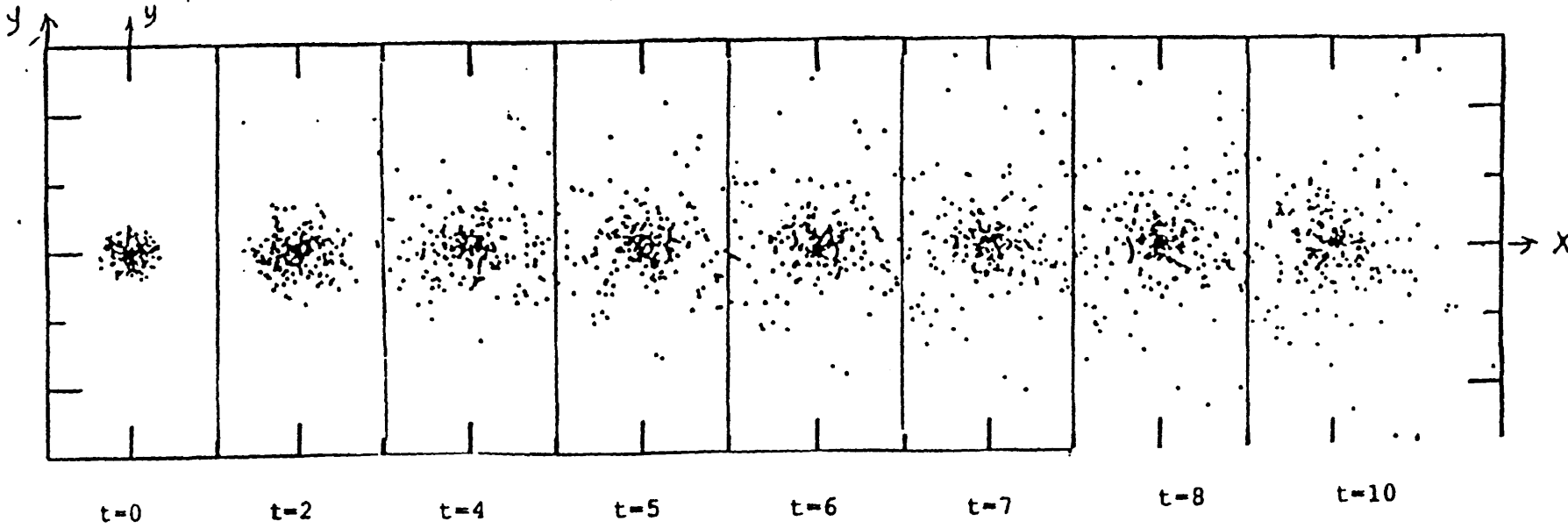
**Fig.3.** The structure of system for the model 4 ( $q_0=0.75, M=1$ ).

**Fig.4a.** The structure of system for the model 5 in the XY-plane ( $q_0=0.90, M=1$ ).

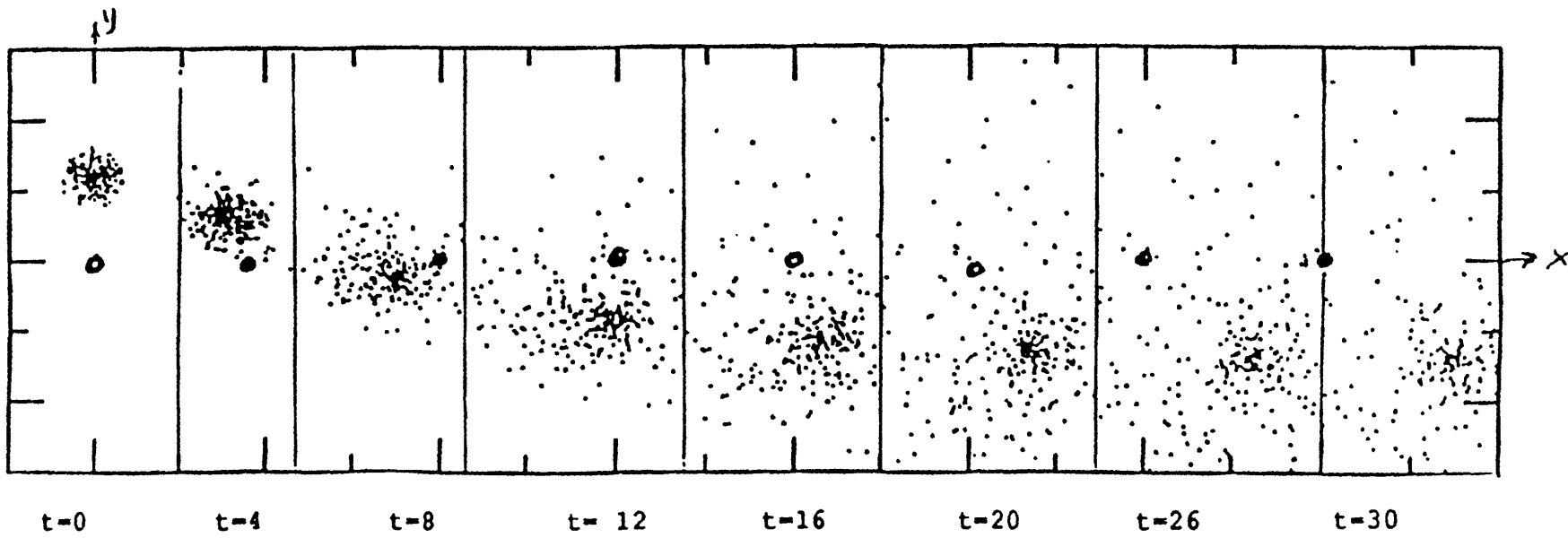
**Fig.4b.** The structure of system for the model 5 in the XZ-plane ( $q_0=0.90, M=1$ ).

**Fig.5.** The structure of system for the model 6 ( $q_0=0.50, M=5$ ).

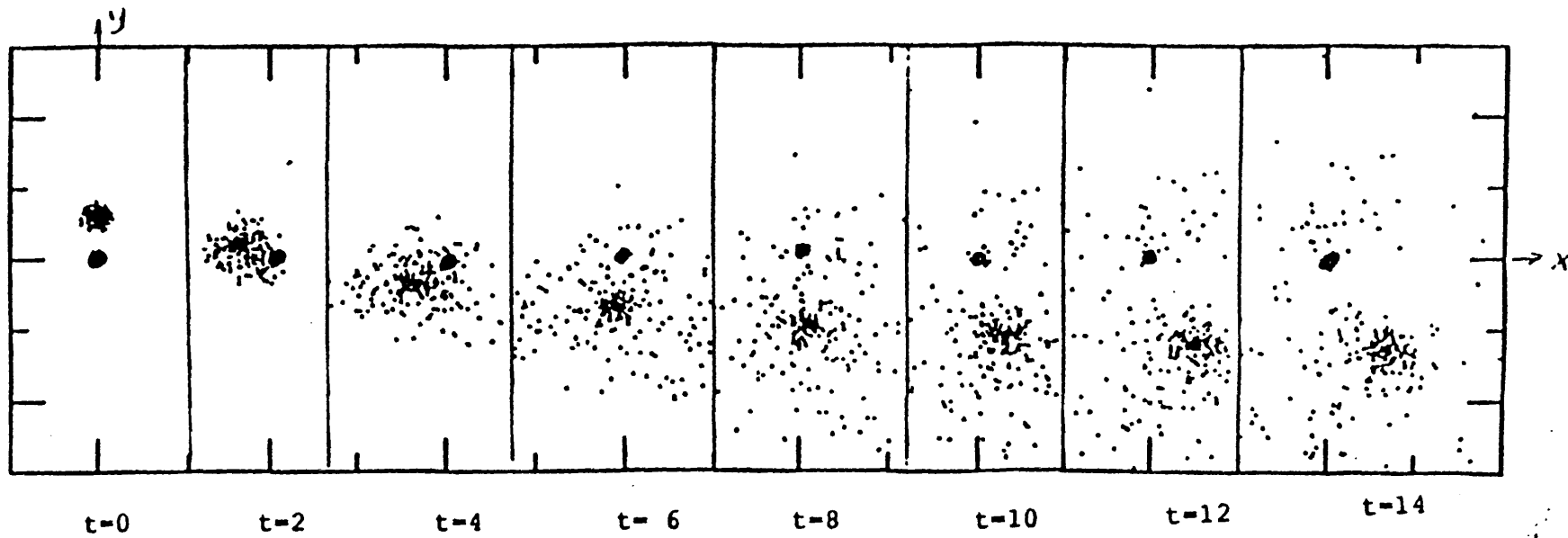
**Fig.6.** The structure of system for the model 9 ( $q_0=0.50, M=10$ ).



The model 1

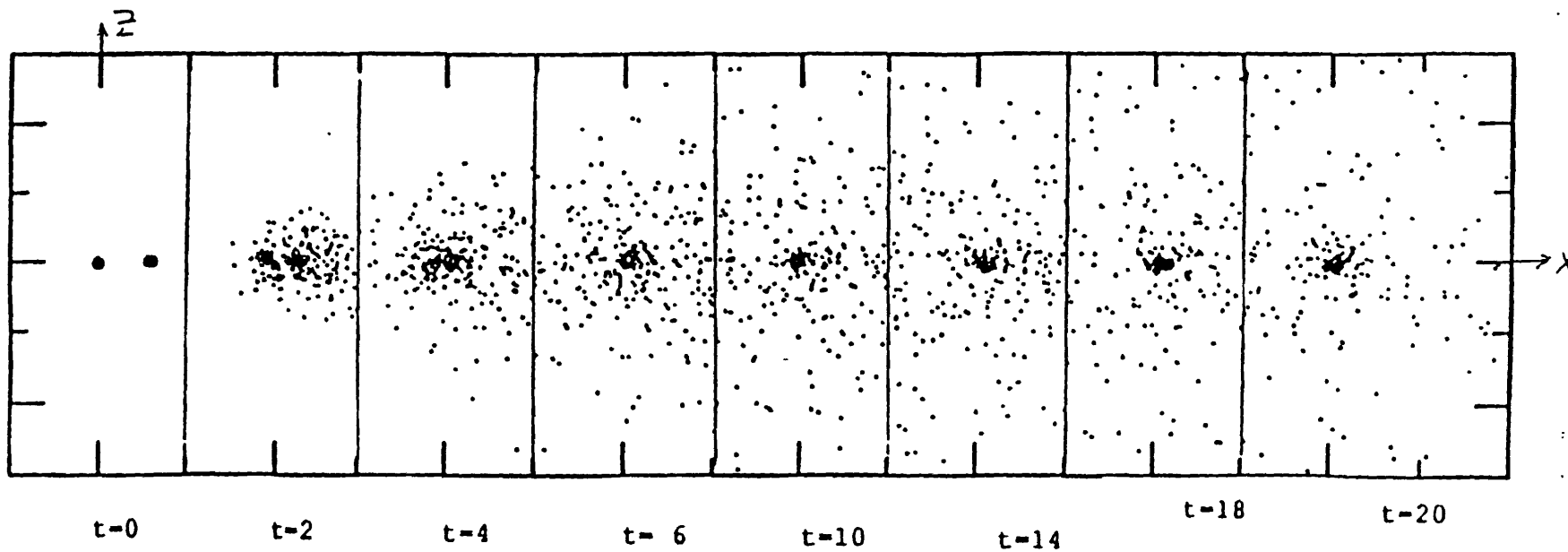


The model 3

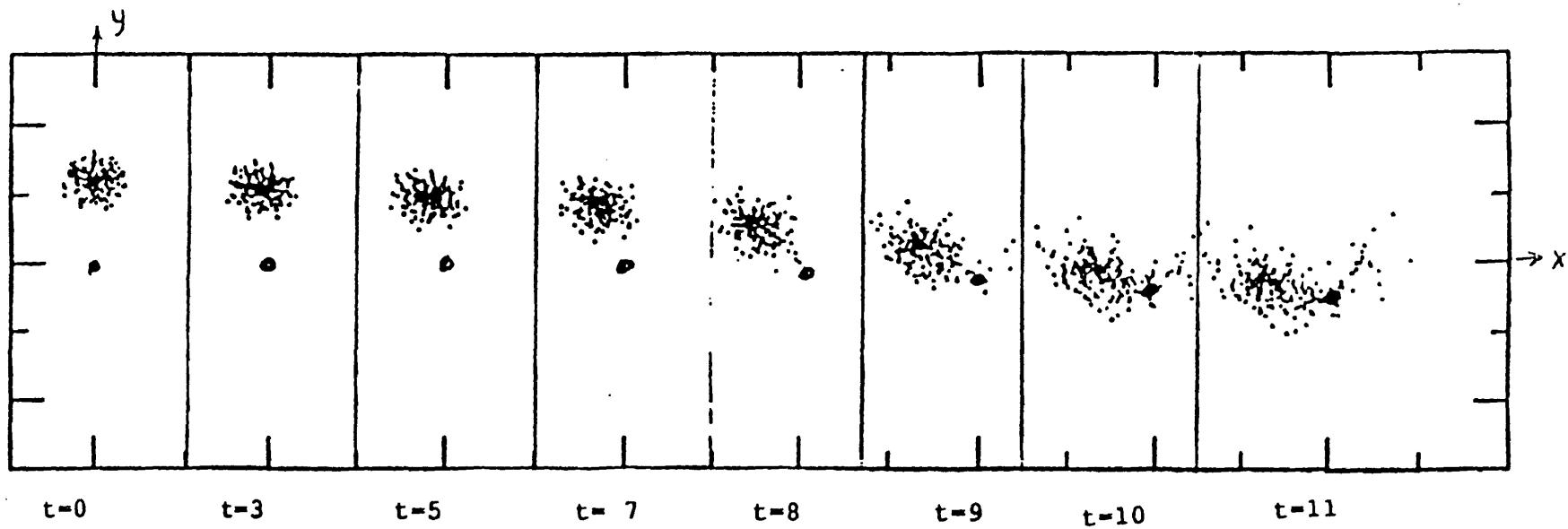


The model 4

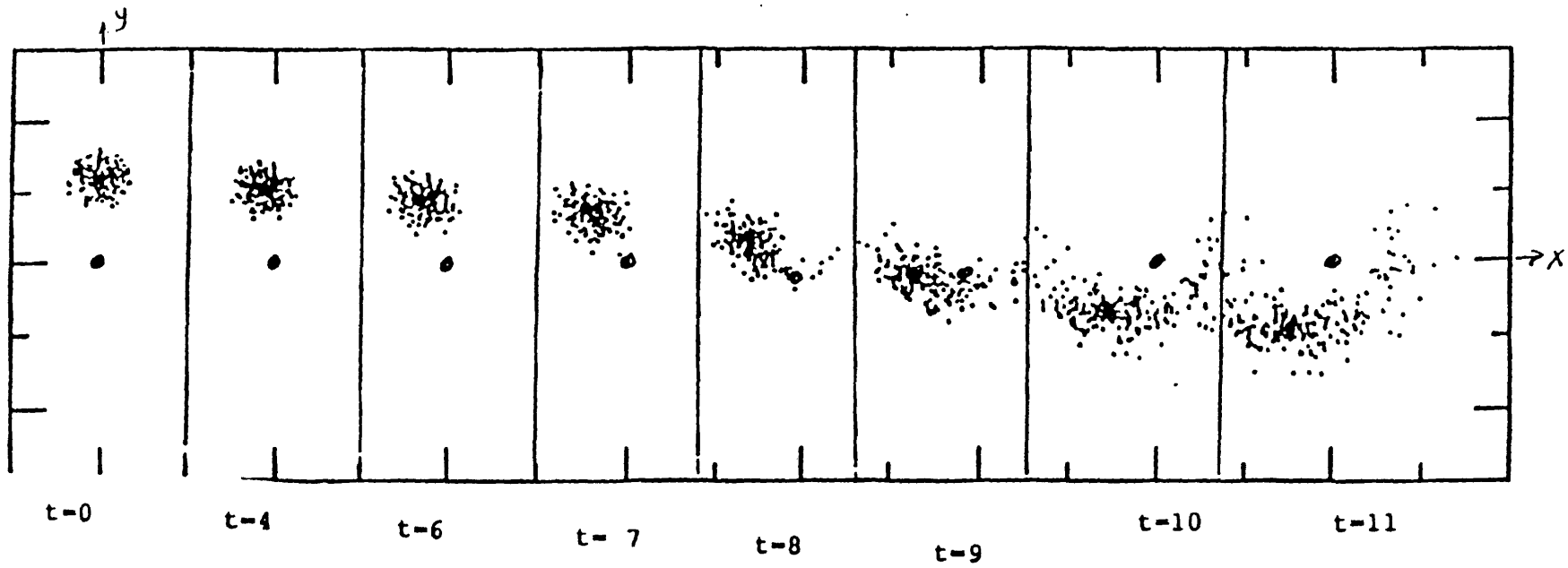




The model 5b



The model 6



The model 9